Chemical Bulletin of "Politehnica" University of Timisoara, ROMANIA
Series of Chemistry and Environmental Engineering
Chem. Bull. "POLITEHNICA" Univ. (Timisoara) *Volume 60(74), 2, 2015*

Highly Efficient Removal of Amoxicillin from Water by Magnetic Graphene Oxide Adsorbent

S.E. Moradi

Faculty of Science, Islamic Azad University-Sari Branch 48164-194, Iran, e-mail: er_moradi@hotmail.com

Abstract: In the present work, graphene oxide (GO) was prepared by hummers method from natural graphite. The structural order and textural properties of the graphene based materials were studied by TEM, XRD, TG-DTA and FT-IR. The adsorption of amoxicillin on GO and magnetite GO with different variable such as: contact time, adsorbent dosage, initial concentration, pH and temperature was investigated. The kinetic studies showed that the adsorption data followed a pseudo second-order kinetic model. The isotherm analysis indicated that the adsorption data can be represented by Langmuir isotherm model.

Keywords: amoxicillin, magnetic graphene oxide, adsorption, Langmuir isotherm

1. Introduction

Personal care products, pesticides and a number of industrial chemicals have been found in infiltrated waters. They come into water sources frequently through discharge from pharmaceutical industries and from urban wastewater treatment plants [1, 2]. Consumption of water contaminated with antibiotics can have numerous contrary effects on humans including acute and chronic toxicity [3, 4]. Amoxicillin, with molecular dimensions of 15.622Å ×18.785Å × 6.645Å [5], is one of the major β-lactam antibiotics because of its high spectrum of activity, high solubility, high rate of absorption, and its stability under acid conditions. Amoxicillin has also been recognized to be hardly degradable, remains as active compound within urine and feces [6, 7]. A number of methods have been tried to remove antibiotics in conventional wastewater treatment plants, including filtration [8], biological processes [9], coagulation [10], flocculation [11] and sedimentation [12]. However, new strategies are required because these have proved to be not very effective.

Adsorption has been considered as an attractive method to eliminate organic contaminants from aqueous solutions because of its simplicity, low cost and insensitivity to toxic pollutants [13-15]. Up to now, numerous researches related to the adsorption of pharmaceuticals onto adsorbent from natural resources e.g. silica [16], clays [17,18], hydrous oxides [19] and soils [20] have been published.

Through the last decade, significance in the use of novel carbon based materials for environmental applications has increased considerably. Between all carbon nanomaterials, graphene oxide (GO) is well-studied and it has proven to have superior mechanical strength, good chemical stability, high specific surface area (theoretically 2600 m^2/g), low density, and superior mechanical strength [21–24], which makes it a suitable material for environmental applications. Graphene oxide has different kind of oxygen functional groups (epoxy, carboxyl and hydroxyl) on the surface, consequently electrostatic interaction with organic material become greater [25]. Moreover graphite oxide is able to adsorb number of chemicals onto the benzene ring by the strong π–π interaction [26].

Recently, magnetic loaded adsorbents have proven to be highly efficient and easily separable [27, 28]. Fe3O4 magnetic nanoparticles (MNPs) are either physically adsorbed onto GO [29, 30] or covalently attached to it [31, 32]. Magnetite GO have been applied to targeted drug carriers [33], magnetic resonance imaging [34], and pollutant removal [35]. Good stability and the large surface area of magnetite GO made it capable for adsorption of organic pollutants [36].

In this work, the adsorption behavior of carbon based adsorbents (GO, and magnetite GO) based on equilibrium adsorption capacity, pH effect, kinetic studies and thermodynamic factors for amoxicillin were examined. It has been found that the adsorption capability of magnetite GO for amoxicillin molecules is much higher compared to that of GO and other novel adsorbents. Langmuir and Freundlich adsorption isotherms were studied to explain the sorption mechanism.

2. Experimental

2.1. Materials

Graphite powder (<20 micron) was purchased from Sigma-Aldrich, Germany and used as-received. H_2SO_4 (>99%), hydrochloric acid (AR grade), H_2O_2 (30% (w/v)), KMnO4 (>99%), iron (II) chloride tetrahydrate ($FeCl_2 \cdot 4H_2O$), iron (III) chloridehexahydrate ($FeCl_3 \cdot 6H_2O$) and ammonia solution (NH_4OH) were all purchased from Sigma-Aldrich ((St. Louis, MO, USA).

Amoxicillin (Fig. 1), which consists of two fundamentals parts that contain β-lactam inner and the side chain called d-hidroxiphenilglicin, ($C_{16}H_{19}N_3O_5S$, MW= 365.4) was purchased from Sigma-Aldrich, USA (98% purity, St. Louis, MO, USA). A stock solution of 100 mg/L of Amoxicillin was prepared in double distilled water and the experimental solutions of the desired concentration were obtained by successive dilutions.

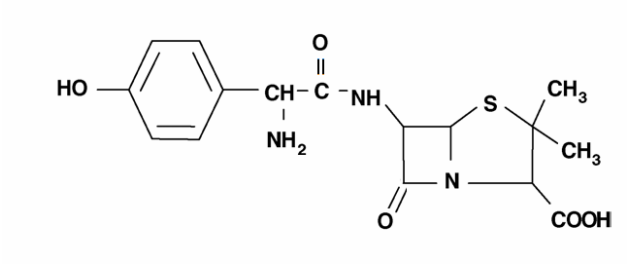

Figure 1. Molecular structure of amoxicillin

2.2. Synthesis of GO adsorbent

GO was synthesized from expandable graphite using a modified Hummers' method [37]. 1 g of graphite powder was added to 23 mL of concentrated H_2SO_4 in an ice bath. $KMnO_4$ (3 g) was then added slowly with stirring and cooling to keep the temperature of the reaction mixture below 293 K. The temperature of the reaction mixture was increased and maintained at 308 K for 30 min. When 46 mL of deionized water was added slowly to this mixture temperature was increased to 371 K. After 15 minutes 140 mL of deionized water was added followed by 10 mL of 30% H_2O_2 solution. The solid product was separated by centrifugation. It was washed repeatedly with 5% HCl solution until the sulfate ions are removed and then washed with distilled water repeatedly until it becomes free of chloride ions. The product was then filtered and washed 3–4 times with acetone to make it moisture free and the residue thus obtained was dried in an oven at 338 K overnight. The GO was suspended in water and exfoliated through ultrasonication for 3 h.

2.3. Chemical modification of GO by magnetite nanoparticles

Magnetite GO was obtained by method as described by Thu et. al [38]. In a typical synthesis procedure (magnetite GO), 99.5 mg of $FeCl_2.4H_2O$ and 270.5 mg of $FeCl_3 \cdot 6H_2O$ (molar ratio 1:2) were dissolved in 30 mL of deionized water under sonication for 5 min. This mixture was added to 30 mL of GO and thoroughly stirred for 30 min at room temperature. To this solution, 2 mL of NH_4OH was then added drop-wise to reach a mild alkaline pH (10–11). The mixture turned from light brown to dark brown and finally black color, indicating the formation of Fe_3O_4. The suspension was then heated to 353 K and kept at that temperature for1 h. Upon the completion of the reaction, the as-prepared Magnetite GO were magnetically separated and washed with water several times to obtain clean products. Alternatively, Magnetite GO can be collected by centrifugation or paper filtration.

2.4. Characterization

The morphology and surface structure of GO and magnetite GO were examined by X-ray diffraction (XRD, Philips Xpert MPD, Co Kα irradiation, λ = 1.78897A˚), JEM-2100F transmission electron microscope (TEM) and The Fourier transform infrared spectra (DIGILAB FTS 7000) instrument under attenuated total reflection (ATR) mode using a diamond module. The composition and thermal properties of GO and magnetite GO were determined by TGA with a PL Thermal Sciences; model PL-STA using a heating rate of 10 K/min from room temperature to 1073 K under Ar. The measurements were conducted using approximately 3 mg samples and then weight retention/temperature curves were recorded.

2.5. Adsorption studies

A stock solution of 100 mg/L of amoxicillin was prepared by dissolving an appropriate amount of the amoxicillin in ultra-pure water (18 MΩ cm) derived from a Milli-Q plus 185 water purifier. 0.01 g magnetite GO adsorbent was added to 100 mL of amoxicillin solutions (10-50 mg/L) and the mixture was shaken on a rotary shaker at 150 rpm for different times. After adsorption, the suspension was centrifuged at 10,000 rpm for 10 min. The amount of amoxicillin adsorbed was calculated by subtracting the amount found in the supernatant liquid after adsorption from the amount of amoxicillin present before addition of the adsorbent by UV-Vis spectrophotometer (UV mini 1240 shimadzu). Absorbance was measured at wavelength (λ_{max}) 275.5 nm for determination of amoxicillin content. Calibration experiments were done separately before each set of measurements with amoxicillin solution of different concentrations. The effect of temperature on the adsorption of amoxicillin by magnetite GO was investigated by incubating the samples under different temperature conditions (303 K, 313 K, 323 K and 333 K). To study the influence of pH on adsorption of amoxicillin by magnetite GO, the initial pH of magnetite GO was adjusted from 4 to 10 using NaOH or HCl aqueous solution. All tests were performed in duplicate to ensure reproducibility of the results; the mean of these two measurements was taken to represent each evaluation. Calculations of amounts of adsorption of amoxicillin onto magnetite GO were based on adsorption capacity (Eq. (1)).

$$q_e = \frac{(C_o - C_e)V}{W} \qquad (1)$$

where q_e (mg/g) is equilibrium adsorption capacity, C_o and Ce (mg/L) are the initial and equilibrated amoxicillin concentrations, respectively. V (L) is the volume of solution and W (mg) is the adsorbent mass.

2.6. Adsorption kinetics of amoxicillin

For sorption kinetics, a series of 250 mL flask containing 0.01 g of magnetite GO and 100 mL of amoxicillin solution at concentration 100 mg/L was prepared. The mixtures were continuously shaken at 303 K and 150 rpm. Samples were taken at different time intervals and filtered using 0.2 lm Millipore membrane filters and the filtrates were analyzed for amoxicillin concentration. The adsorption capacity (q_t, mg/g) at any time, t was calculated using the following equation. (Eq. (2))

$$q_t = \frac{(C_o - C_t)V}{W} \quad (2)$$

where C_t (mg/L) is the amoxicillin concentrations at time *t*.

2.7. Reproducibility and accuracy of the results

All batch isotherm experiments were replicated two times and the blanks were run in parallel to establish accuracy, reliability and reproducibility. All glassware was presoaked in a 5% HNO_3 solution, rinsed with deionized water and oven-dried. Blanks were run and corrections applied, if necessary. Each batch adsorption experiment was conducted triplicate and the data shown are the average values. The individual values were generally within 5%.

3. Results and Discussion

3.1. Characterization of the GO and magnetite GO samples

As shown in Fig. 2a, the broad and relatively weak diffraction peak at 2Θ=10.5° (d=0.87 nm), which corresponds to the typical diffraction peak of graphene oxide adsorbent, is attributed to the (002) plane. The XRD patterns of magnetite GO showed 2Θ = 29.86°, 35.41°, 43.39°, 53.83°, 57.14°, 62.79°, respectively (Fig. 2b), suggesting the presence of magnetic phase in the composites.

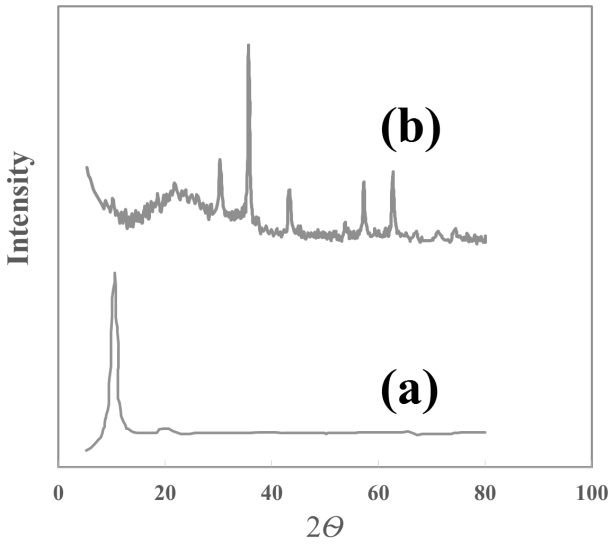

Figure 2. XRD pattern of (a) GO and (b) magnetite GO

Representative TEM image of the obtained magnetite GO is showed in Fig. 3. a. It can be seen that Fe_3O_4 nanoparticle have been coated on the GO surface consistently. It is observed that the size of the magnetite GO was about 17 nm with narrow distribution (Fig. 3. b).

The FTIR spectra of GO and magnetite GO are shown in Fig. 4. Fig. 4.a, shows the presence of the oxygen-containing functional groups. The peaks at 1380, 1630 cm^{-1} correspond to C-OH stretching, C=C stretching mode of the sp^2 carbon skeletal network, respectively, while peaks located at 1730 and 3270 cm^{-1} correspond to C=O stretching vibrations of the COOH groups and O-H stretching vibration, respectively [39]. After modification, three representative peaks of the amide carbonyl group for magnetite GO at 1647 (–CONH amide band I), 1533 (–NH amide band II), and 1455 cm^{-1} (C–N stretch of amide) appeared (Fig. 4.b), implying that Fe_3O_4 nanoparticles were linked to GO surface by covalent bonding [40].

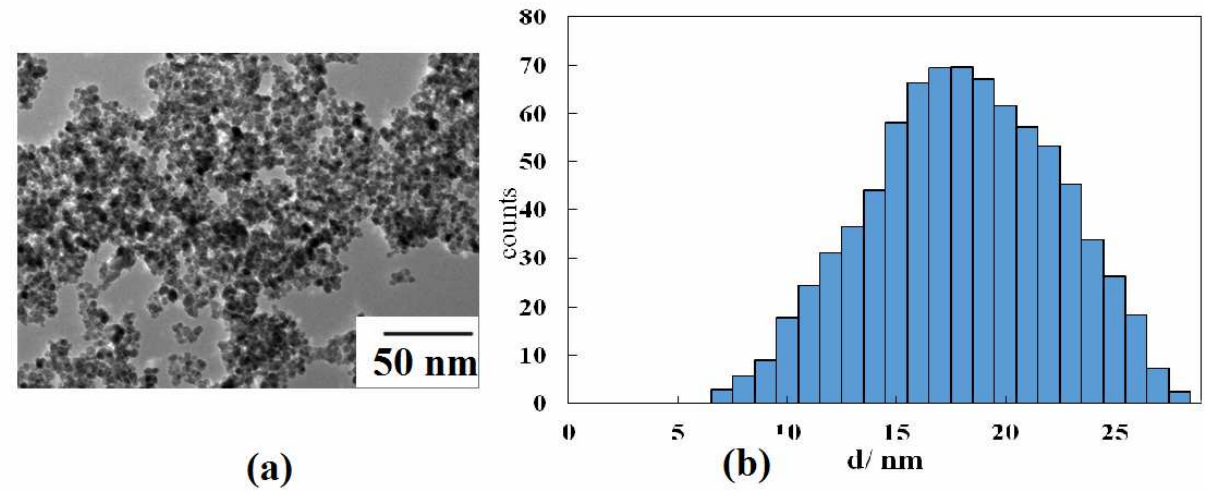

Fig.ure 3. (a) TEM photographs and (b) histogram of particle size distribution of magnetite GO sorbent

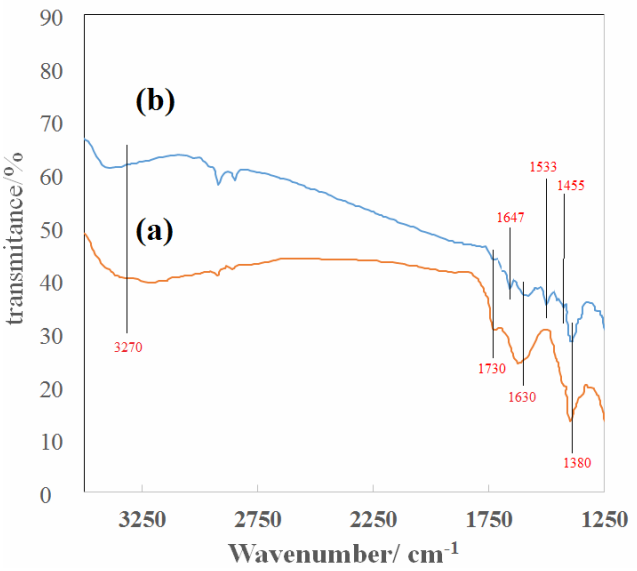

Figure 4. The FT-IR spectra of (a) GO and (b) magnetite GO samples

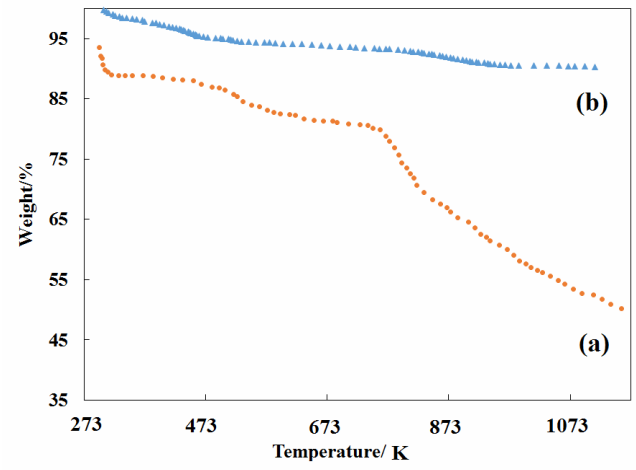

Figure 5. TGA curves of (a) GO and (b) magnetite GO

The TGA was also performed on GO and the magnetite GO adsorbents to find the Fe_3O_4 contents, the structure and thermal stability of the magnetite GO and the graphene oxide (Fig. 5. a and Fig.5 b)). The GO adsorbent shows two major mass loss at 473 and 858 K with 9% and 30% weight loss, respectively. They are related to the elimination of oxygen-containing groups of graphene oxide and oxidation of carbon, respectively. For magnetite GO it is clear that the thermal stability is much higher than pristine GO. Two weight losses at 723 K and 753 K are assigned to the loss of the residual solvent and the breakdown of the CONH group conjugated with Fe_3O_4 nanoparticles of the magnetite GO, respectively. The same result has been previously resulted.

3.2. Adsorption studies

3.2.1. Effect of contact time and initial concentration

Experiments were conducted for various time intervals to determine duration required to reach adsorption equilibrium. Experiments showed that the amount of adsorbed dye gradually increased with the rise of contact time. As follows from Fig. 6, the resultant equilibrium time amounts to 150 min.

Amoxicillin solutions at different initial concentration (10, 20, 50 mg/L) were treated with 0.1 g/L of GO and magnetite GO. Figure 6 shows the effect of varying amoxicillin concentrations against the amount of amoxicillin adsorbed. The amount of amoxicillin equilibrium adsorption removal increases with an increase in initial solution concentration from 91 to 272 mg/g for GO and 130 to 465 mg/g for magnetite GO. This is because of the fact that by increasing the concentration of amoxicillin in solution the availability of amoxicillin at the adsorbent interface also increases. When the surface active sites of adsorbent are covered fully, the extent of adsorption reaches a limit resulting in saturated adsorption.

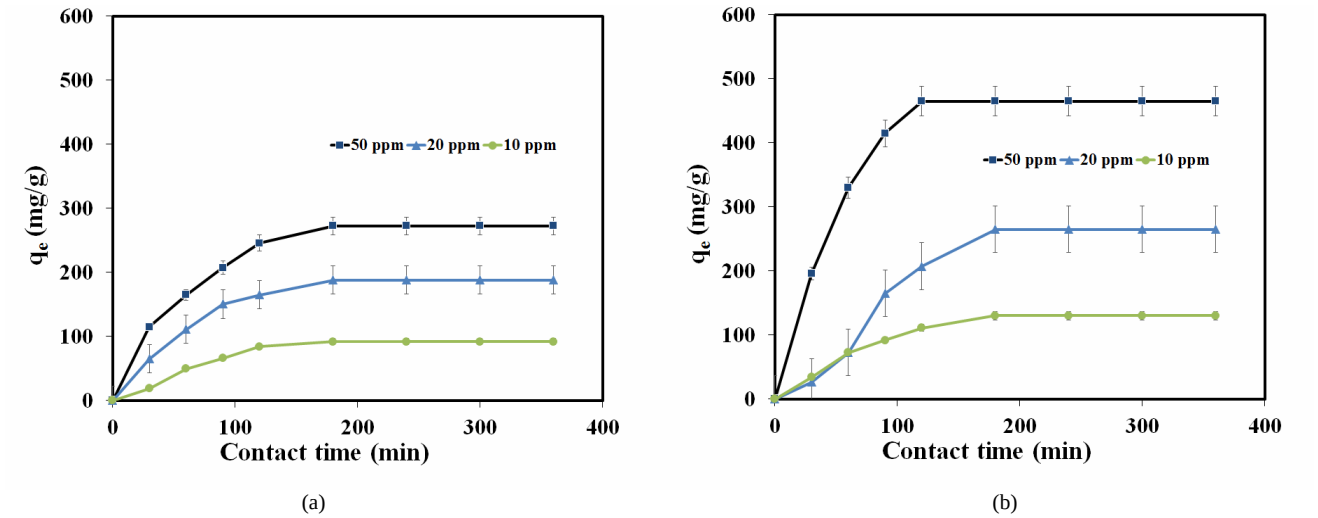

Figure 6. Effect of contact time and initial concentration on removal of amoxicillin by (a) GO (b) magnetite GO ([amoxicillin] =10-50 mg/L, agitation speed = 150 (rpm), adsorbent dosage = 0.1 g/L, temperature = 303 K, pH=6)

3.2.2. Effect of adsorbent dose

Adsorbent dosage is an essential factor influencing adsorption processes meanwhile it determines the adsorption capacity of an adsorbent for a given initial concentration of the adsorbate at the operating conditions. The effect of magnetite GO on removal of amoxicillin was studied in range of 0.05–2.0 g/L. Fig. 7 showed that as adsorbent dosage increased from 0.05 to 0.1 g/L, the adsorption capacity is increased but the removal percent is decreased. It is ascribed to an increase in the adsorptive surface area and the availability of more binding sites. At higher adsorbent dosages significant increase in removal percent of dye is not happening. Consequently, 0.1 g/L adsorbent dosage was chosen as optimum dosage for further analysis.

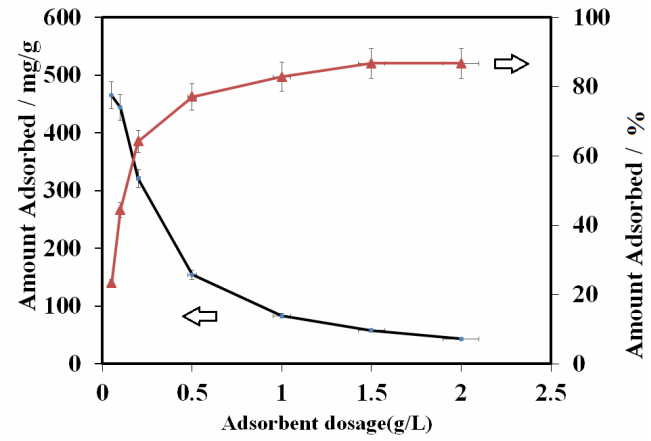

Figure 7. Effect of magnetite GO dosage on the adsorption of amoxicillin. ([amoxicillin] =50 mg/L, agitation speed = 150 (rpm), contact time = 3 h, temperature = 303 K, pH=6)

3.2.3. Effect of solution pH on amoxicillin adsorption capacity

pH is an important factor in controlling the adsorption of pollutant onto adsorbent, which affects the surface charge of the adsorbent and the degree of ionization of the adsorbate. In order to find out the effect of pH, 10 mg of the grapheme oxide the and magnetic grapheme oxide sorbents were treated separately with 50 mL of 50 mg/L amoxicillin at various pH values (from 2 to 12) accompanied by mild shaking at 303 K for 3 h. Fig. 8 shows the effect of pH on adsorption of amoxicillin by GO and magnetite GO. In the pH range up to 6, it was found that the adsorption capacity of amoxicillin increased with increasing the solution pH [41]. This could be attributed to the fact that the protonation of carbonyl groups of amoxicillin became insignificant at high pH. At relative high range of pH values the reduced protons corresponding to the increased negative active sites on GO adsorbent promotes the electrostatic and H-bonding interactions with amoxicillin functional groups. Moreover, GO can form a strong π- π interaction with amoxicillin because of the large delocalized π-electron system of graphene [42]. But after pH 6 the adsorption capacity reduces with increases in pH values. It is because of the fact that, at higher pH's the surface charge of adsorbent get more and more negative and repulsion forces between magnetite GO and amoxicillin cause a decrease in amoxicillin adsorption. Despite pH 6 is optimum value of pH, at very low and very high pH still good adsorption for amoxicillin has been shown, it because of the fact that the π- π interaction is not depend on pH of solution and magnetite GO can interact with amoxicillin by π- π mechanisem.

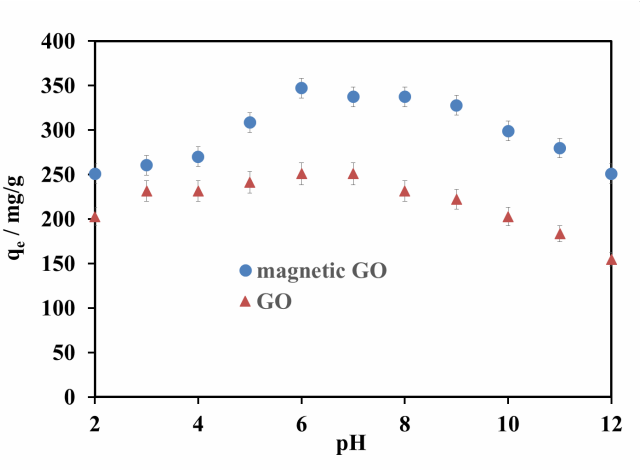

Figure 8. Adsorption of amoxicillin on GO and magnetite GO as a function of pH (adsorbent dosage= 0.1 g/L, [amoxicillin] =50 mg/L, agitation speed = 150 (rpm), temperature = 303 K)

3.2.4. Adsorption kinetics

The kinetic data was fitted with two commonly used pseudo-first-order [43] and pseudo-second-order models [43] to obtain the rate of the reaction and their non-linear forms are represented as given below (Eq. (3) and Eq. (4)) [43]:

$$\log(q_e - q_t) = \log q_e - \frac{k_1 t}{2.303} \quad (3)$$

$$\frac{t}{q_t} = \frac{1}{k_2 q_e^2} + \frac{t}{q_e} \quad (4)$$

where k_1 (L/min) and k_2 (g/mg.min) are the pseudo-first-order and pseudo-second-order rate constants, respectively. The kinetic adsorption data were fitted to Eq. (3) and Eq. (4), and the calculated results are listed in Table 1. The correlation coefficients (R^2) for pseudo-second-order model are all higher than for pseudo-first-order model (Fig. 9) and the experimental data fit to the pseudo-second-order model better than pseudo-first-order model. The results indicate that chemical adsorption might be the rate-limiting step [43]. From the pseudo-first-order and pseudo-second-order models, the rate of amoxicillin adsorption on magnetite GO was determined to be 0.015 L/min and 0.071 g/mg.min and the predicted q_e values were 355.88 and 368.41 mg/g, respectively (Table 1).

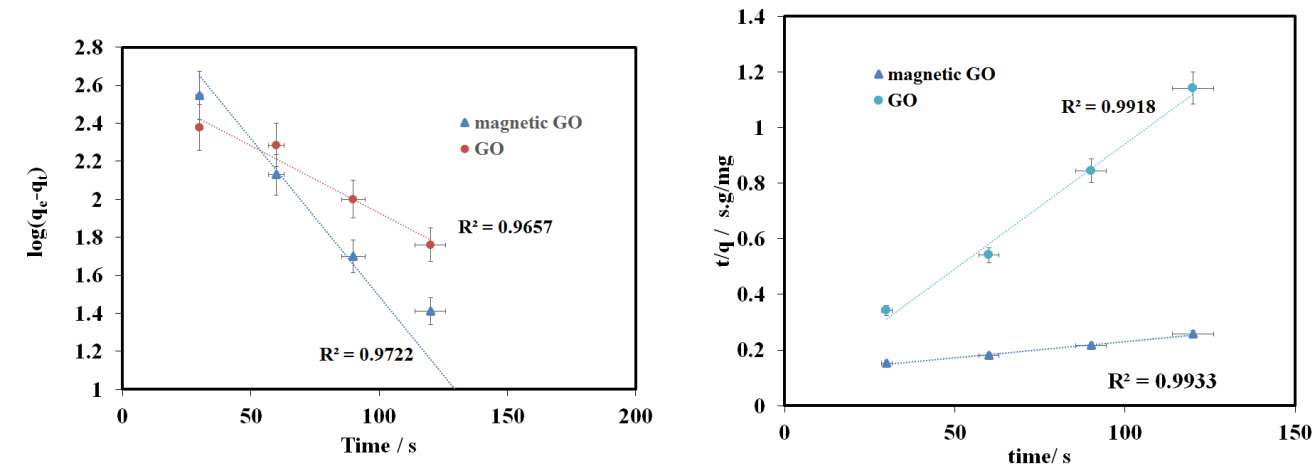

(a) (b)

Figure 9. (a) pseudo-first-order and (b) pseudo-second-order dynamic models for amoxicillin by GO and magnetite GO. ([amoxicillin] = 50 ppm, agitation speed = 150 (rpm), adsorbent dosage = 0.1 g/L, temperature = 303K, pH=6)

TABLE 1. Parameter values of the kinetics models fitting to the experimental results for amoxicillin by GO and magnetite GO. ([amoxicillin] = 50 ppm, agitation speed = 150 (rpm), adsorbent dosage = 0.1 g/L, temperature = 303 K, pH=6)

Adsorbent	Pseudo-first order model			Pseudo-second order model		
	k_1 (L/min)	R^2	q_e (mg/g)	k_2 (g/mg.min)	R^2	q_e (mg/g)
GO	0.011	0.9657	191.64	$2.14*10^{-5}$	0.9918	224.87
magnetite GO	0.015	0.9722	355.88	$2.96*10^{-5}$	09933	368.41

TABLE 2. Thermodynamic parameters for adsorption of amoxicillin on GO and magnetite GO. ([amoxicillin] = 50 ppm, agitation speed = 150 (rpm), adsorbent dosage = 0.1 g/L, temperature = 303-333 K, pH=6)

T(K)	C_e (mg/L)	q_e (mg/g)	Kc	ΔG° (kJ/mol)	ΔH° (kJ/mol)	ΔS° (J/mol.K)
303	13.7	363.3	26.5	-8.2	8.7	55.9
313	12.5	375.1	30.01	-8.8		
323	11.7	383.4	32.77	-9.4		
333	10.8	392.3	36.32	-9.9		

3.2.5. Adsorption thermodynamics

The adsorption isotherms of amoxicillin on GO and magnetite GO at four different temperatures (303-333) are investigated. It has shown that the adsorption of amoxicillin on GO and magnetite GO is promoted at higher temperatures. Thermodynamic parameter related to the adsorption process i.e., free energy change (ΔG, kJ/mol) for adsorption amoxicillin on GO and magnetite GO was calculated using Eq. (5) [44].

$$\Delta G = -RT\ln K_L \qquad (5)$$

where R is the universal gas constant (8.314 J/mol.K), T is the temperature and K_L is Langmuir constant (L/mol) obtained from the plot of C_e/q_e versus C_e. The calculated ΔG value was found to be −328 kJ/mol. The negative value of free energy change indicated the spontaneous nature of sorption and confirmed affinity of graphene based adsorbents for the amoxicillin removal from water [44, 45]. The enthalpy change ΔH and ΔS can be obtained from the van't Hoff equation, Eq. (6)

$$\ln K_L = \frac{\Delta S}{R} - \left(\frac{\Delta H}{R} \times \frac{1}{T}\right) \qquad (6)$$

A linear plot of ln K_L versus 1/T is obtained from the model. The enthalpy change (ΔH) and entropy change (ΔS) can be calculated from the slope and intercept of the van't Hoff plot, respectively. As shown in Table 2, the positive enthalpy change (ΔH) suggests that the adsorption of this work is an endothermic reaction.

3.2.6. Adsorption isotherms

Equilibrium adsorption isotherm is the one of the most essential design parameter expresses how the adsorbate interacts with the adsorbent. The sorption mechanism and affinity of the adsorbent could be clarified by modeling of isotherms by different equilibrium models [46, 47]. In this study, the two most common isotherms, Langmuir and Freundlich models [48], were used to describe the experimental adsorption data. Langmuir model assumes monolayer adsorption onto a surface which consists of finite number of active sites having a uniform energy [49].

The linear form of Langmuir isotherm equation is given as Eq. (7).

$$\frac{C_e}{q_e} = \frac{C_e}{Q_\circ} + \frac{1}{(Q_\circ * b)} \quad (7)$$

where, Ce (mg/L) is equilibrium concentration of adsorbate; qe (mg/g) is the amount of adsorbate adsorbed at equilibrium; Qo (mg/g) is maximum monolayer adsorption capacity; b (L/mg) is Langmuir constant.

According to Freundlich model, it was often applicable to describe the models of multilayer absorption onto the surface of heterogeneous sites with different bond energy. The equation of Freundlich model is given as following Eq. (8).

$$\log q_e = \log K_F + \frac{1}{n} \log C_e \quad (8)$$

where qe is the amount of adsorbate adsorbed at equilibrium (mg/g), Ce is the residual concentration of adsorbate in bulk solution at equilibrium (mg/L); KF and 1/n are the constants related to adsorption of adsorbent and intensity of the adsorption, respectively.

These two Models fit to equilibrium adsorption results of amoxicillin on GO and magnetite GO were assessed based on the values of the determination coefficient (R^2) of the linear regression plot. The obtained experimental data were fit with these two models. The Langmuir and Freundlich isotherms were found to be linear over the whole concentration range studied with higher R^2 values (>0.98) In addition, the Langmuir and Freundlich model parameters for the adsorption of amoxicillin on GO and magnetite GO adsorbents are listed in Table 3. The maximum monolayer capacities of amoxicillin, q_{max}, obtained from Langmuir model are 280.8 and 372.4 mg/g for GO and magnetite GO, respectively. It was important that the maximum adsorption capacity of the magnetite GO is much larger than that of pristine GO. This value is even larger than amoxicillin adsorption amounts in various absorbents [50–56] (Table. 4), clearly indicating the magnetic graphene oxide presented in current research is outstanding candidate in designing magnetically separable adsorbent for drug pollution removing from wastewater.

The critical features of the Langmuir isotherm can be expressed by a dimensionless constant separation factor R_L given by following relation that can be used to determine the possibility of adsorption in a specified concentration range over adsorbents Eq. (9) [57].

$$R_L = \frac{1}{1 + bC_\circ} \quad (9)$$

The calculated R_L values at different initial amoxicillin concentration were in the range of 0.025–0.058, which lie between 0 and 1, confirming that the adsorption of amoxicillin on magnetite GO was favorable [57].

4. Conclusion

Adsorption of amoxicillin onto graphene oxide and magnetic graphene oxide was performed to find the optimum conditions. The consequences of experiments presented that at pH = 6, an amount of adsorbent of 0.1 g/L and a time of 3 h were optimal conditions for the removal of 50 mg/L of amoxicillin. The pseudo-second-order kinetic model best described the adsorption behavior of amoxicillin onto GO and magnetite GO. GO and magnetite GO exhibited good kinetic characteristics (equilibrium time 3 h) and high adsorption capacity for amoxicillin. Equilibrium adsorption isotherm was fitted well with Langmuir model.

TABLE 3. Langmuir and Freundlich constants for adsorption amoxicillin removal on GO and magnetite GO

	Langmuir			Freundlich		
Adsorbent	q_m (mg/g)	b (L/mg)	R^2	K_F (mg/g)	n (L/mg)	R^2
GO	280.8	0.0138	0.9992	125.2	6.7	0.9871
Magnetite GO	372.4	0.0113	0.9995	341.6	8.4	0.9772

TABLE 4. The q_m values of different adsorbents used for amoxicillin removal

Adsorbent	q_m (mg/g)	Reference
active carbon	261.8	[50]
chitosan beads	8.71	[51]
NH_4Cl-induced activated carbon	438.6	[52]
magnetic multi-walled carbon nanotubes	0.23	[53]
activated carbon nanoparticles prepared from vine wood	2.69	[54]
organobentonite	26.18	[55]
magnetic Fe_3O_4@C nanoparticles	142.85	[56]
GO	280.8	This work
magnetite GO	372.4	This work

REFERENCES

1. Ollers S., Singer H.P., Fassler P. and Muller S.R., *J. Chromatogr. A*, 911(2), **2001**, 225-234.
2. Rizzo L., Meric S., Guida M., Kassinos D. and Belgiorno V., *Water Res.*, 43(16), **2009**, 4070-4078.
3. Zuccato E., Castiglioni S., Bagnati R., Melis M. and Fanelli R., *J. Hazard. Mater.*, 179, **2010**, 1042-1048.
4. Mojica E.R.E. and Aga D.S., *Encycl. Environ. Health*, 28, **2011**, 97-110.
5. Boles M.O., Girven R.J. and Gane P.A.C., *Acta Crystallogr. B.*, 34, 1976, 461-466.
6. Andreozzi R., Canterino M., Marotta R. and Paxeus N., *J. Hazard. Mater.*, 122, **2005**, 243-250.
7. Jara C.C., Fino D., Specchia V., Saracco G. and Spinelli P., *Appl. Catal., B*, 70, **2007**, 479-487.
8. Choi K.J., Kim S.G. and Kim S.H., *J. Hazard. Mater.*, 151, **2008**, 38-43.
9. Zhou P., Su C., Li B. and Qian Y., *J. Environ. Eng. Sci.*, 132, **2006**, 129-136.
10. Choi K.J., Kim S.G. and Kim S.H., *Environ Technol.*, 29(3), **2008**, 333-342.
11. Homem V. and Santos L., *J. Environ. Manage*, 92, **2001**, 2304-2347.
12. Rohricht M., Krisam J., Weise U., Kraus U.R. and During R.A., *CLEAN – Soil, Air, Water*, 37(8), **2009**, 638- 641.
13. Haghseresht F., Nouri S. and Lu G.Q., *Carbon*, 41, **2003**, 881-892.
14. Ayranci E., Hoda N. and Bayram E., *J. Colloid Interface Sci.*, 284, **2005**, 83-88.
15. Haydar S., Fero-García M.A., Rivera-Utrilla J. and Joly J.P., *Carbon*, 41, **2003**, 387-395.
16. Figueroa R.A. and MacKay A.A., *Environ. Sci. Technol.*, 39, **2005**, 6664-6671.
17. Figueroa R.A., Leonard A. and MacKay A.A., *Environ. Sci. Technol.*, 38, **2004**, 476-483.
18. Pils J.R.V. and Laird D.A., *Environ. Sci. Technol.*, 41, **2007**, 1928-1933.
19. Gu C. and Karthikeyan K.G., *Environ. Sci. Technol.*, 39, **2005**, 2660-2667.
20. Bui T.X. and Choi H., *Chemosphere*, 80, **2010**, 681-686.
21. Novoselov K.S., Geim A.K., Morozov S.V., Jiang D., Zhang Y. and Dubonos S.V., *Science*, 306, **2004**, 667-669.
22. Lee C., Wei X., Kysar J.W. and Hone J., *Science*, 321, **2008**, 385-388.
23. Freitag M., Steiner M., Martin Y., Perebeinos V., Chen Z.H., Tsang J.C. and Avouris P., *Nano Lett.*, 9, **2009**, 1883-1888.
24. Balandin A.A., Ghosh S., Bao W., Calizo I., Teweldebrahn D., Miao F. and Lau C.N., *Nano Lett.*, 8, **2008**, 902-907.
25. Gao Y., Li Y., Zhang L., Huang H., Hu J., Shah S.M. and Su X., *J. Colloid Interface Sci.*, 368, **2012**, 540-546.
26. Cai X., Tan S., Lin M., Xie A., Mai W., Zhang X., Lin Z., Wu T. and Liu Y., *Langmuir*, 27, **2011**, 7828-735.
27. Xu C., Wang X., Zhu J.W., Yang X.J. and Lu L.D., *J Mater Chem*, 18, **2008**, 5625-5629.
28. Ambashta R.D. and Sillanpaa M., *J. Hazard. Mater.*, 180, **2010**, 38-49.
30. Yao Y., Miao S., Liu S., Ma L.P., Sun H. and Wang S., *Chem. Eng. J.*, 184, **2010**, 326-332.
31. Xie G., Xi P., Liu H., Chen F., Huang L. and Shi Y., *J. Mater. Chem.*, 22, **2012**, 1033-1039.
32. Namazi H. and Adeli M., *Eur. Polym. J.*, 39, **2003**, 1491-1500.
33. Yang X., Zhang X., Ma Y., Huang Y., Wang Y. and Chen Y., *J. Mater. Chem.*, 19, **2009**, 2710-2714.
34. Cong H.P., He J.J., Lu Y. and Yu S.H., *Small*, 6, **2010**, 169-173.
35. Qu S., Huang F., Yu S.N., Chen G. and Kong J.L., *J. Hazard. Mater.*, 160, **2008**, 643-647.
36. Xie G.Q., Xi P.X., Liu H.Y., Chen F.J., Huang L., Shi Y.J., Hou F.P., Zeng Z.Z., Shao C.W. and J. Wang, *J. Mater. Chem.*, 22, **2012**, 1033-1039.
37. Hummers W.S. and Offeman R.E., *J. Am. Chem. Soc.*, 80, **1958**, 1339-1339.
38. Thu T.V. and Sandhu A., *Mater. Sci. Eng., B*, 189, **2014**, 13-20.
39. Ai L.H., Zhang C.Y. and Chen Z.L., *J. Hazard. Mater.*, 19, **2007**, 4559-4563.
40. Depan D., Girase B., Shah J.S. and Misra R.D.K., *Acta Biomater.*, 7, **2011**, 3432-3445.
41. Fan L., Luo C., Sun M., Qiu H. and Li X., *Colloids Surf., B*, 103, **2013**, 601-607.
42. Dreyer D., Park S., Bielawski C. and Ruoff R., *Chem Soc Rev*, 39, **2010**, 228-240.
43. Ho Y.-S., *Water Res.*, 40, **2006**, 119-125.
44. Xu J., Wang L. and Zhu Y., *Langmiur*, 28, **2012**, 8418-8425.
45. Zhao G.X., Li J.X. and Wang X.K., *Chem. Eng. J.*, 173, **2011**, 185-190.
46. Inbaraj B.S., Chiu C.P., Ho G.H., Yang J. and Chen B.H., *J. Hazard. Mater.*, 137, **2006**, 226-234.
47. Ho Y.S. snd McKay G., *Process Biochem.*, 38, **2003**, 1047-1061.
48. Rao M., Parwate A.V. and Bhole A.G., *Waste Manage.*, 22, **2002**, 821-830.
49. Jain A.K., Gupta V.K., Bhatnagar A., Jain S., Suhas A., *J. Indian Chem. Soc.*, 80, **2003**, 267-270.
50. Feng Q., Wang X., Jia Y., Ning P., *Appl. Mech. Mater.*, 295, **2013**, 1235-1239.
51. Adriano W.S., Veredas V., Santana C.C. and Goncalves L.R.B., *Biochem. Eng. J.*, 27, **2005**, 132-137.
52. Moussavi G., Alahabadi A., Yaghmaeian K. and Eskandari M., *Chem. Eng. J.*, 217, **2013**, 119-128.
53. Fazelirad H., Ranjbar M., Taher M.A. and Sargazi G., *J. Ind. Eng. Chem.*, 21, **2015**, 889-892.
54. Pouretedal H.R. and Sadegh N., *Journal of Water Process Engineering*, 1, **2014**, 64-73.
55. Zha S.X., Zhou Y., Jin X. and Chen Z., *J. Environ. Manage.*, 129, **2013**, 569-576.
56. Kakavandi B., Esrafili A., Mohseni-Bandpi A., Jafari A.J. and Kalantary R.R., *Water Sci Technol.*, 69, **2014**, 147-155.
57. Ai L., Li L.M. and Li L., J. *Chem. Eng. Data.*, 56, **2011**, 3475-3483.

Received: 01 September 2015
Accepted: 20 November 2015